Adsorption (2009) 15: 365–380
DOI 10.1007/s10450-009-9187-4

Adsorptive separation in the enhancement of butene dehydrogenation

Saleh Rawadieh · Vincent G. Gomes

Received: 30 April 2008 / Accepted: 12 May 2009 / Published online: 3 June 2009

Abstract Fixed-bed columns containing solid catalysts and adsorbents were employed for simultaneous reaction and separation. The models developed for butene dehydrogenation reaction were validated with experimental data. The model was then employed for variable bed configurations with and without the effect of pressure and vacuum swing reaction (PSR and VSR). The models for the mass and momentum transfer in the catalyst bed and adsorber were solved using orthogonal collocation within the method of lines. The reactor/separator performances were tested for beds with varying numbers of layers of catalysts and adsorbents arranged sequentially. The reaction columns behaved as reactor/separators in series. As the number of layers increased, a homogeneous distribution of the catalyst and adsorbent was approached in the limit. These configurations with variable catalyst/adsorbent distributions were investigated in terms of product purity, selectivity, conversion, recovery and yield. Improved reactor performance was observed with pressure and vacuum swing separation systems and in particular with close to well-mixed reactor/separator configurations.

Keywords Adsorption · Separation · Butene dehydrogenation · Pressure swing reaction · Vacuum swing reaction

Notation

b	langmuir adsorption coefficient, kg/mol
C	gas phase concentration, mol/cm^3
D_z	axial dispersion coefficient, m^2/s
G	purge to feed ratio
K	mass transfer coefficient, s^{-1}
L	bed length, m
$L_{C,k}$	length of kth catalyst layer
$L_{A,k}$	length of kth adsorbent layer
Nc	number of components
P	pressure, atm
Pe	Peclet number $= \frac{ul}{D_z}$
q	concentration in the adsorbed phase, mol/kg
r_{rxn}	rate of reaction, mol/s.kg
t	time, s
u	inlet gas velocity
$\overline{v}$	dimensionless interstitial fluid velocity $= \frac{v}{u}$
x_{CA}	catalyst/adsorbent volume ratio
x_i	dimensionless solid-phase mole fraction $= \frac{\overline{q}_i}{q_s}$
y	gas mole fraction
z	variable for bed axial distance

Greek letters

α_i	dimensionless mass transfer coefficient $= \frac{k_i L}{u}$
ε	bed voidage
ρ	density, kg/m^3
υ_i	stoichiometric coefficient of component i
τ	dimensionless time $= \frac{tu}{L}$
ξ	mass capacity factor $= \rho_{ads}(\frac{1-\varepsilon}{\varepsilon})(\frac{q_{is}}{c_0})$

Subscripts

Ads, A	adsorbent
Cat, C	catalyst
$feed$	feed stream
i	denotes gas species
B_d	butadiene
B	1-butene

S. Rawadieh · V.G. Gomes (✉)
School of Chemical and Biomolecular Engineering,
The University of Sydney, Sydney, Australia
e-mail: v.gomes@usyd.edu.au

H_2	hydrogen
H	high pressure
L	low pressure
s	saturation

Superscripts

*	equilibrium condition

1 Introduction

A substantial number of industrially important chemical reactions are limited by equilibrium conversion of reactants within a feed and product mix. An important recent innovation is to combine the reaction and separation steps in a single unit operation known as reactive separation or integrated reactive separation and the process unit is called a multifunctional reactor. This combination has been recognized by process industries as having possible favourable economics and an important means for implementing process intensification. Typical examples are reactive distillation and absorption, membrane reactors and adsorptive reactors (Armor 1998; Stankiewicz and Moulijn 2000; Krishna 2002; Stankiewicz 2003; Aida and Silveston 2005).

Pressure swing adsorption (PSA) has been extended to chemical reactors using separation of products/reactants during chemical conversion. A mixture of catalysts and sorbents are loaded in the reactor vessel and operated under a pressure-swing cycle. Such a reactor has been termed as a periodic separating reactor or a pressure-swing reactor, PSR (Vaporciyan and Kadlec 1987; Carvill et al. 1996; Gomes 2004, 2005). Adsorptive reactors have recently attracted much interest (Lu and Rodrigues 1993, 1994; Gomes and Fuller 1994, 1996; Yongsunthon and Alpay 1998a, 1998b; Hufton et al. 1999; Ding and Alpay 2000; Sheikh et al. 2001; Gomes and Yee 2002; Xiu et al. 2002a, 2002b; Rawadieh and Gomes 2007) due to their significant economic potential. However, there is lack of information regarding the optimal catalyst and adsorbent configurations within such reactors and their effects on reactor performance.

In PSR, a mixture of catalyst and adsorbent may be arranged in either a homogeneous or a heterogeneous configuration. In homogeneous units, the catalyst and the adsorbent are mixed uniformly while heterogeneous units are formed by dividing the unit into separate regions: the catalyst-packed region followed by the adsorbent-packed bed region. In such units, the strongly adsorbed components are held by the adsorbents in order to attain enhanced reactor performance by shifting the reaction equilibrium in the desired direction.

By packing the bed with several layers of catalyst and adsorbent sequentially, the PSR column becomes reactors in series. The overall performance of the PSR may therefore depend on the arrangement (Lu and Rodrigues 1993, 1994; Rawadieh and Gomes 2007). The advantage of this structure over the mixed structure is that the adsorbent is not completely mixed with the catalyst and thus the catalyst can be readily separated from the adsorbent when there is a need for treatment or reactivation of catalyst during a major plant turnaround. In this work, multiple heterogeneous layers will be investigated besides the two limiting configurations: fully homogeneous and simply heterogeneous.

Rawadieh and Gomes (2007) have tested fixed beds with varying numbers of layers of catalysts and adsorbents which were arranged sequentially. As the number of layers increased, a homogeneous distribution of the catalyst and adsorbent was approached in the limit. These configurations with variable catalyst/adsorbent distributions were investigated for propene metathesis reaction, in terms of product purity, conversion, recovery and productivity. Improved reactor performance was observed with a pressure swing separation system and in particular with close to well-mixed reactor/separator configurations.

Butadiene is used primarily as a monomer in the production of a range of polymers and co-polymers. It is also used in the production of several intermediate chemicals. The largest single use for butadiene is in the production of styrene-butadiene rubber (SBR) which, in turn, is principally used in the manufacture of tyres. Other familiar products that are derived from butadiene include telephones, computer casings, carpet backings, nitrile rubber hoses, footwear, road surfaces and neoprene items, such as wetsuits. World demand for butadiene has increased fairly consistently between 2001 and 2006 and up to 2010, demand is expected to grow at a rate of three percent per year (Ullmann 2007).

The production of 1,3-butadiene is carried out by dehydrogenation of 1-butene in a fixed-bed catalytic reactor. Typically, the feed stream is diluted and the reactor operates at 700–900 K to achieve high conversions. Due to the high temperature associated with the reaction process, coking reactions also occur, resulting in catalyst deactivation by fouling. The catalyst life is usually extended by regeneration of the catalyst by burning off the coke. Due to the interest of this reaction and the associated coke problems, a number of workers have studied its reaction and deactivation kinetics (Acharya and Hughes 1990; Brito et al. 1995; Sheikh et al. 2001).

Dumez and Froment (1976) experimentally determined the kinetics of 1-butene dehydrogenation using a Langmuir-Hinshelwood approach, including coke deposition and catalyst decay for a chromia-alumina catalyst. The catalyst deactivation was found to depend on the coke deposited on the catalyst from both 1-butene and 1,3-butadiene via the following scheme:

$$\begin{tikzcd} C_4H_8 \arrow[rr, shift left] \arrow[dr, "r_{C1}"] & & C_4H_6 + H_2 \arrow[ll, shift left] \arrow[dl, "r_{C2}"'] \\ & \text{Coke} & \end{tikzcd} \tag{1}$$

With surface reaction on dual sites as the rate determining step, the kinetics for the above reaction is given as follows (Dumez and Froment 1976):

$$r_1 = \frac{1.826 \times 10^7 \exp(-29236/R_g T)(p_B - \frac{p_H p_{Bd}}{K_C})}{(1 + 1.8727 p_B + 3.593 p_H + 38.028 p_{Bd})^2} \times \exp(-42.12 C_C) \tag{2}$$

where r_1 is the reaction rate for dehydrogenation (kmol/kg_cat.h), C_C is the percentage weight coke content of the catalyst (kg_coke/kg_cat), p_B, p_H and p_{Bd}, are the partial pressures (atm) of butene, butadiene and hydrogen, respectively, K_C is chemical equilibrium constant (atm), T is the temperature (K), and R_g is the universal gas constant (J/mol.K).

One of the advantages associated with incorporating separation and reaction in the same unit is the reduction of deactivation rate of catalysts (William and Kulprathipanja 2002; Aida and Silveston 2005). With negligible coking and at equilibrium the rate of reaction expression equates zero, thus K_C can be defined in terms of partial pressures (or concentrations) of the reaction species at equilibrium (eqm).

$$K_C = \frac{P_{H,eqm} P_{Bd,eqm}}{P_{B,eqm}} \tag{3}$$

Equation (3) can be rewritten in terms of the equilibrium conversion X_{eqm}, total pressure P (atm) and the feed mole fraction of butene $y_{B,f}$:

$$K_C = \frac{X_{eqm}^2 y_{B,f}}{(1 - X_{eqm})(1 + X_{eqm} y_{B,f})} P \tag{4}$$

Following estimation of K_C from Gibbs free energy at a specified temperature, (6) can be solved for X_{eqm}. It can be clearly seen that increase of dilution of the reactant and low operating pressure result in high conversion.

2 Reactor-separator model

A dynamic model accounting for isothermal and isobaric operations was developed to describe both the fixed-bed reactor (FBR) and the sorption enhanced reactor processes. A Langmuir model was used to describe the adsorption equilibria of butadiene, and a linear driving force (LDF) model was used for the mass transfer of the adsorbent. Other principal model assumptions can be summarised as: axially dispersed plug flow, perfect gas behaviour, no radial concentration, and a catalyst/adsorbent packing of uniform voidage and particle size.

Based on the above assumptions, component mass balances for the packed-bed reactor can be written in dimensionless form as:

$$\frac{1}{P}\frac{\partial (P y_i)}{\partial \tau} = \frac{1}{Pe}\frac{\partial^2 y_i}{\partial \bar{z}^2} - \frac{\partial (\bar{v} y_i)}{d\bar{z}} - \rho_{ads}\left(\frac{1-\varepsilon}{\varepsilon}\right)\left(\frac{q_{is}}{c_0}\right)\frac{\partial x_i}{\partial \tau} + \upsilon_i \bar{r}_{rxn} \tag{5}$$

The overall mass balance for gas-phase is given:

$$\frac{\partial \bar{v}}{\partial \bar{z}} = \frac{1}{P}\frac{\partial P}{\partial \tau} - \xi \sum_{i=1}^{Nc} \frac{q_{is}}{q_{is,ref}} \frac{\partial x_i}{\partial \tau} + \sum \upsilon_i \bar{r}_{rxn} \tag{6}$$

where i denotes butene, butadiene, hydrogen and inert. The semi-empirical correlation proposed by Edwards and Richardson (1968) was used to estimate the axial dispersion coefficient D_z.

The LDF model is adopted in dimensionless form to describe the mass-transfer of adsorbates:

$$\frac{\partial x_i}{\partial t} = \alpha_i (x_i^* - x_i) \tag{7}$$

where $\alpha_i = \frac{k_i L}{u}$.

The value of LDF coefficient, k_i, was originally estimated from the diffusional time constant (D_e/r^2) based on laboratory experiments (Sheikh et al. 2001) for 1.78×10^{-4} m diameter adsorbents at 763 K. For larger particles (diameter 0.003 m), suitable for industrial PSR, we corrected the diffusional time constant (Ruthven et al. 1994) as follows:

$$\left(\frac{r_1}{r_2}\right)^2 = \left(\frac{0.0015}{0.000079}\right)^2 \approx 20^2$$

The inter-bed pressure dynamics for the variable pressure steps are estimated using a linear dynamic pressure (Sereno and Rodrigues 1993; Malek and Farooq 1997; Xiu et al. 2002b).

$$\frac{\partial P}{\partial \tau} = \begin{cases} 0 & \text{for adsorption step} \\ -(P_H - P_L)/\tau_{BL} & \text{for blowdown step} \\ 0 & \text{for desorption step} \\ (P_H - P_L)/\tau_{PR} & \text{for pressurisation step} \end{cases} \tag{8}$$

The extended Langmuir equation for butadiene adsorption is given by:

$$x_1^* = \frac{b_i c_0 y_i}{1 + \sum_i b_i c_0 y_i} \tag{9}$$

Initial conditions

$y_{i,}(\bar{z},0)=0, \qquad x_i=0$

The final distributions of concentrations, pressure along the adsorptive reactor column for one step are the initial conditions for the next step.

Boundary conditions for the four steps

PSR steps	Gas-phase concentration	
	$Z/L=0$	$Z/L=1$
Adsorption	$\frac{1}{Pe}\frac{\partial y_i}{\partial \bar{z}}=-\bar{\upsilon}\vert_{z=0}(y_{i,f}-y_i\vert_{z=0})$	$\frac{\partial y_i}{\partial \bar{z}}\vert=0$
Blowdown	$\frac{\partial y_i}{\partial \bar{z}}=0$	$\frac{\partial y_i}{\partial \bar{z}}\vert=0$
Desorption	$\frac{\partial y_i}{\partial \bar{z}}\vert=0$	$\frac{1}{Pe}\frac{\partial y_i}{\partial \bar{z}}\vert=-\bar{\upsilon}\vert_{z=L}(y_{z=L,adsorption}-y_i\vert_{z=L})$
Pressurisation	$\frac{1}{Pe}\frac{\partial y_i}{\partial \bar{z}}=-\bar{\upsilon}\vert_{z=0}(y_{i,f}-y_i\vert_{z=0})$	$\frac{\partial y_i}{\partial \bar{z}}\vert=0$
	Velocity	
Adsorption	$\bar{\upsilon}=1$	$\frac{\partial \bar{\upsilon}}{\partial \bar{z}}=0$
Blowdown	$\frac{\partial \bar{\upsilon}}{\partial \bar{z}}=0$	$\bar{\upsilon}=0$
Desorption	$\frac{\partial \bar{\upsilon}}{\partial \bar{z}}=0$	$\bar{\upsilon}=G$
Pressurisation	$\bar{\upsilon}=f(P)$	$\frac{\partial \bar{\upsilon}}{\partial \bar{z}}=0$

The stoichiometric coefficients for 1-butene (B), hydrogen (H) and butadiene (Bd) are $\upsilon_B=-1$, $\upsilon_E=-1$, $\upsilon_{Bd}=-1$, respectively

The model given above was used to simulate 1-butene dehydrogenation for the following cases: reaction without adsorption (plug flow reactor or PFR), reaction with adsorption and no PSR cycles and reaction with PSR cycles. Comparisons between the PSR and PFR were performed using a favourable pressure for PFR, i.e., low pressure operation. To assess the reactor/separator performance, the following indicators were defined:

Conversion

$$=\frac{\text{mole of butene fed} - \text{moles of butene in column exits}}{\text{moles of butene fed to the column}}$$

$$=\frac{\sum\int^t (n^* v^* C_B \partial t)_{\text{streams}}}{\int^t (\upsilon_{feed}{}^* C_{B,feed} \partial t)} \tag{10}$$

Where n is $+1$ for outgoing and -1 for ingoing streams

$$\text{Yield}=\frac{\text{moles of butadiene in column exits}}{\text{moles of butene fed to the column}}$$

$$=\frac{\sum\int^t (n^* v^* C_{Bd} \partial t)_{\text{streams}}}{\int^t (\upsilon_{feed}{}^* C_{B,feed} \partial t)} \tag{11}$$

Butadiene purity

$$=\frac{\text{moles of butadiene collected in desorption outlet stream}}{\text{moles of (hydrogen + butadiene + butene) in desorption outlet stream}} \tag{12}$$

Hydrogen purity

$$=\frac{\text{moles of hydrogen collected in adsorption outlet stream}}{\text{moles of (hydrogen + butadiene + butene) in adsorption outlet sream}} \tag{13}$$

Butadiene recovery

$$=\frac{\text{moles of butadiene collected in desorption stream}}{\text{Total moles of butadiene produced by the catalyst}} \tag{14}$$

Hydrogen recovery

$$=\frac{\text{moles of hydrogen collected in adsorption stream}}{\text{Total moles of hydrogen produced by catalyst}} \tag{15}$$

3 Results and discussions

3.1 Plug flow reactor without adsorption

A continuous plug flow reactor PFR process was first simulated with reaction only (no separation). Equation (2) was used as the rate of reaction assuming negligible coking. Our simulation results for PFR were compared with experimental data (Sheikh et al. 2001). Conversion is mainly compared with experimental data as there was considerable cracking of the product, 1,3-butadiene, resulting in low selectivity and yield of butadiene.

The model predictions and experiments show that in PFR, the conversion of 1-butene decreases with feed flowrate (Fig. 1). Good agreement between simulations and experiments are noted. Our fixed-bed model was used in conjunction with the PSR for the same conditions employed for the fixed-bed reactor, i.e. low pressure operation.

Since the model predictions agreed with the available experimental data, we simulated the performance of a scaled-up PFR of 30 cm length, 1.75 cm diameter and feed flow rate

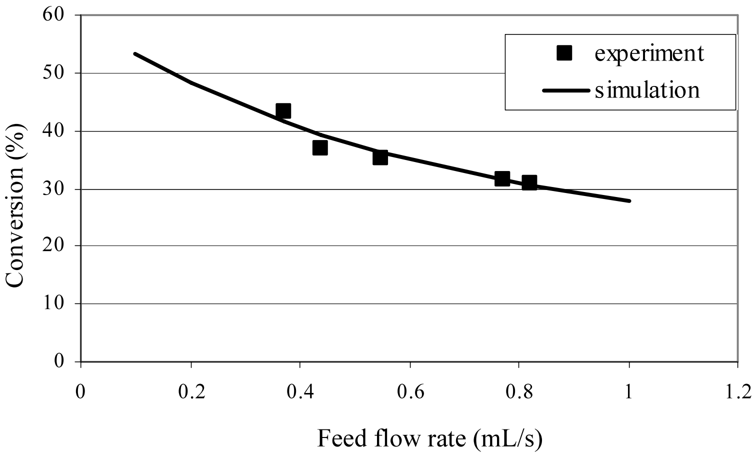

Fig. 1 Comparison of simulation and experimental results (Sheikh et al. 2001) for PFR performance with fresh catalyst after 10 minutes (no catalytic deactivation), $P = 2$ bar, $T = 763$ K. $L = 11.7$ cm, $D = 0.2$ cm, $y_{B,f} = 0.01$. Feed flow rates are at (STP) Feed flow rate (mL/s)

Table 1 Reactor bed characteristics

	Unit	Column
Column inside radius	m	0.0175
Bed length	m	0.60
Temperature	K	763
Catalyst density (Sheikh et al. 2001)	kg/m^3	1006
Adsorbent density (Sheikh et al. 2001)	kg/m^3	741
Bed voidage	m^3/m^3	0.40
Particle diameter	m	0.003
Viscosity (Reid et al. 1987)	kg/m.s	1.3×10^{-3}
Peclet number (*Pe*) (Edwards and Richardson 1968)	–	98.7
Molecular diffusivity (Reid et al. 1987)	m^2/s	2.3×10^{-5}
Adsorption isotherm parameters		
b_{Butene}	L/mol	0, (25)
$b_{Butadiene}$	L/mol	50
q_{Butene}	mol/kg	0, (1.0)
$q_{Butadiene}$	mol/L	1.0

of 400 mL/min (25°C, 1 atm) with 0.25 1-butene feed mole fraction as the base case. The conversion in PFR was noted to be 10.4% and the butadiene purity was 10.6% at 763 K and 1 atm.

3.2 Adsorptive reactor without the effect of PSR

A packed bed adsorptive reactor with length of 60 cm and diameter of 1.75 cm was assumed to be packed uniformly with an admixture of catalyst and adsorbent. The same amount of catalyst used in the packed bed reactor was used here and with a catalyst-adsorbent volume ratio of (1:1). Simulations were carried out for cases where the selection of adsorbent would affect the performance of the process. The values of adsorption isotherm parameters (Antonucci et al. 1978; Schweich and Villermaux 1982; Lu and Rodrigues 1994) used in the numerical simulations are listed in Table 1. The bracketed adsorption isotherms parameters of butene are used only when butene is considered to be adsorbed. Sheikh et al. (2001) have used chromia-alumina as a catalyst and zeolite KY as an Adsorbent.

In their simulations, Sheikh et al. (2001) assumed that both the forward and backward reactions follow elementary kinetics (16). This assumption is questionable as it does not distinguish between the substantial differences that hydrogen and butadiene partial pressures potentially have on the reaction. The comprehensive kinetics (2), that we used, indicates that the chemisorption coefficient for butadiene (in the denominator) is much greater than that for hydrogen. Thus, a reduction in butadiene partial pressure (through removal via physisorption) will lead increased reaction rate and equilibrium conversion.

$$r = k_f\left(p_B - \frac{p_H p_D}{K_C}\right) \tag{16}$$

Fig. 2 Model predictions of exit mole fractions of 1-butene dehydrogenation species in a uniform admixture of catalyst-adsorbent at 3 atm, 763 K, (**a**): only butadiene is adsorbed, (**b**): only hydrogen is adsorbed, (**c**): butadiene is strongly adsorbed with a medium affinity of butene toward the adsorbent, and, (**d**): hydrogen is strongly adsorbed with a medium affinity of butene toward the adsorbent

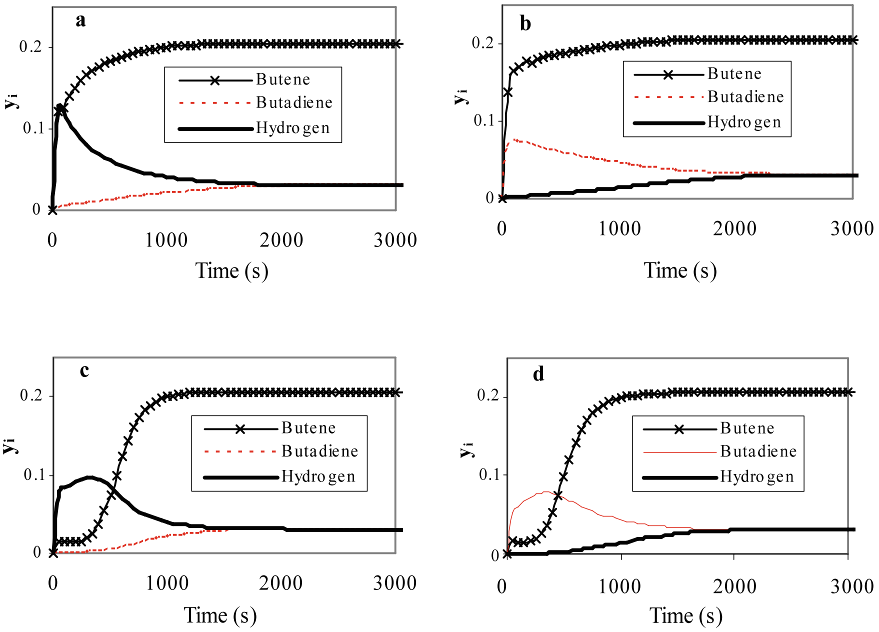

Table 2 Data used for simulating the base case

Variables		Unit	
Feed rate at 25°C and 1 atm	Total	cm^3/min	400
	1-Butene	cm^3/min	100 (25%)
	Inert	cm^3/min	300 (75%)
Feed pressure	atm	3	
Purge pressure	atm	1	
Purge to feed ratio	mol/mol	1	
Adsorption-desorption time	s	200	
Blowdown-pressurization time	s	50	
Catalyst/adsorbent volume ratio	m^3/m^3	1:1	

Figure 2 shows the mole fraction of species with respect to reaction time with four different scenarios (cases). When butadiene (which has an adsorption constant of *38.028* atm^{-1} in the *reaction rate expression*) is selectively removed and the other reaction components have negligible affinity toward the adsorbent (case 1), the conversion of butene was found to be around 13.78% after 5000 seconds. Using the same data but switching the selectivity toward hydrogen (which has an adsorption coefficient of *3.59* atm^{-1}) instead of butadiene, the conversion of 1-butene was found to be 12.80%. These values are given on a cumulative basis over a period of 5000 s (Fig. 2a and b).

The effect of reactant adsorption for the cases mentioned above was investigated with butene having a lower sorption affinity than one of the products, while the other product component has negligible affinity. In such cases, the actual conversion estimation is affected by butene adsorption. Nevertheless, we note the change of exit mole fraction of the product with negligible affinity toward the adsorbent and/or its total mole collected at the column exit over a certain period (i.e., 5000 s). This can be used as both products have similar stoichiometric coefficients. When butadiene is preferentially adsorbed with a medium affinity for 1-butene and negligible affinity for hydrogen (case 3), the production of hydrogen is lower than that without the adsorption of reactant. This can be explained as follows: when there is significant reactant adsorption, lower reactant residence time occurs in the bed as it is adsorbed on the adsorbent and, thus, it will not be available for the reaction (see Fig. 2c). The same behaviour can be seen with the case of hydrogen being preferentially adsorbed with medium affinity of 1-butene and negligible affinity of butadiene (case 4) see Fig. 2d. The production of butadiene is higher in the case of no adsorption of butene is considered. However, the production of butadiene in this case (case 4) is also lower than that for the production of hydrogen in the case where adsorption of reactant is significant (case 3), see Table 3 and Fig. 2c and d.

Table 3 Simulation results for the adsorptive reactors (uniformly-mixed) without the effect of PSR

	Case 1	Case 2	Case 3	Case 4
Conversion (%)	13.7	12.8	–	–
Components	Total moles produced over a reaction time of 5000 s (mmol)			
	Case 1	Case 2	Case 3	Case 4
Hydrogen	96.9	–	89.0	–
Butadiene	–	92.8	–	83.2

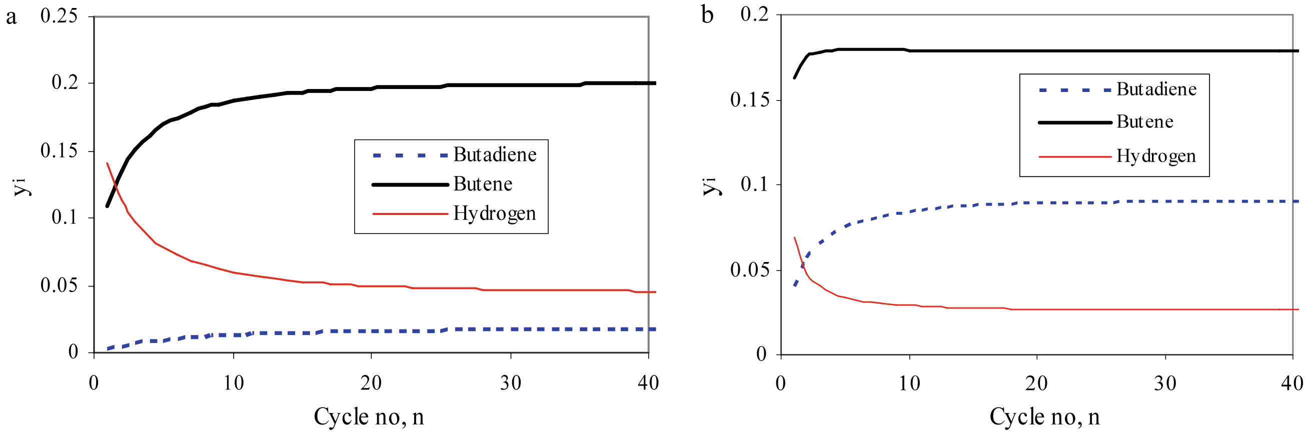

Fig. 3 Model predictions of exit mole fractions in gas-phase as a function of cycle numbers for well-mixed configuration (catalyst:adsorbent = 1:1); (**a**): at the end of adsorption step ($Z/L = 1$), (**b**): at the end of desorption step ($Z/L = 0$)

3.3 Enhanced pressure swing reaction of 1-butene dehydrogenation

We considered a two-bed adsorptive reactor operated based on the Skarstrom cycle configuration of industrial relevance. Since hydrogen affinity toward most of adsorbents is negligible, butadiene is the only component that is preferentially adsorbed relative to 1-butene. Reducing the mole fraction of 1-butene (high conversion) and butadiene (removed by adsorption) in gas phase will result in reducing the catalyst coking as indicated by the kinetics proposed by Dumez and Froment (1976).

The dehydrogenation of butene was simulated in conjunction with pressure swing reactor (PSR) effect. PSR is a cyclic batch process for which adsorption is carried out at a relatively higher pressure and desorption (regeneration) is accomplished at a lower pressure, using part of the product from the adsorption step. During the high pressure adsorption step, the preferentially adsorbed species are retained in the column, leaving the purified raffinate product in the gas phase. During desorption (regeneration), the adsorbed species are removed from the adsorbent, thus regenerating the column for use in the next cycle. Our PSR consists of two-bed with four steps; adsorption/reaction, counter-current blowdown/reaction, counter-current desorption/reaction and co-current pressurisation/reaction. Tables 1 and 2 show the reactor characteristics and the base case operating conditions used in our work.

In butene dehydrogenation PSR, in which butadiene is only adsorbed, the adsorption step is the production step for hydrogen while the purge step is the production step for butadiene. So, in our simulation, we have considered two bases (butadiene in exhaust stream(s) and hydrogen in the production stream) for each performance indicator, i.e. purity and recovery. The performance of the process as a whole was measured by the total butene conversion, which can be readily measured because there is no adsorption of butene on the adsorbent.

3.3.1 PSR performance as a function of cycles

Figure 3a shows simulation results for the exit mole fraction of all species at the end of adsorption/reaction step. Since butadiene is the only component that has affinity to the adsorbent, it is the last component to be detected, and its concentration is the smallest for all cycles. The adsorption of butadiene removes a product from the reactant and changes the equilibrium-based driving force for the reaction. Thus, reducing butadiene concentration in the reaction zone enhances the conversion of butene. During the first cycle, the adsorbent is fresh and its capacity is the maximum resulting in high conversion at that cycle and hence high concentra-

Fig. 4 Concentration (mol/m^3) history in the PSR for the CSS at both ends of the column in well-mixed configuration

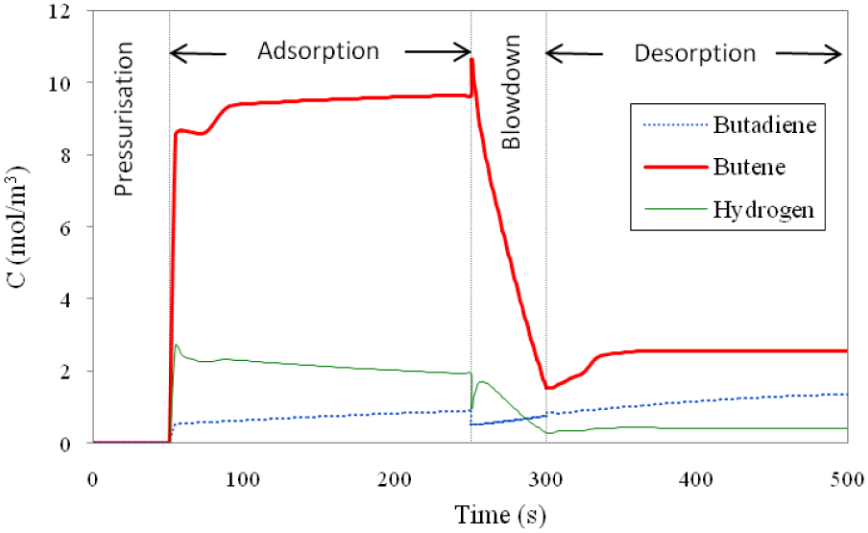

tion of hydrogen. As the cycle number increases the adsorbent capacity decreases until cyclic steady state is attained. The system reaches a cyclic steady state after about 30 cycles with mole fractions of 0.20, 0.045 and 0.018, for butene, hydrogen and butadiene, respectively.

Figure 3b shows our simulations of the exit ($Z/L = 0$) mole fractions of gases at the end of regeneration (purge) step. Butadiene is concentrated at the outlet stream of this step (Fig. 3b). Since part of the product stream from the adsorption/reaction stream is used to regenerate the adsorbent at low pressure, the rates of reaction and desorption processes are dependent on the adsorption step. For the base case, Fig. 3b shows that the mole fraction of hydrogen at the end of desorption/reaction steps decreases with the number of cycles, while the mole fraction of butene and butadiene increases; this is mainly related to the purge to feed flow and the amount of butadiene desorbed. It is expected that purging time, purge to feed ratio and the regeneration pressure play important roles in this process.

3.3.2 PSR performance with time at CSS

Figure 4 shows the exit concentrations ($C_i = P^* y_i$) of species as functions of time during the cyclic steady state or CSS. At the pressurization/reaction step, during the first 50 seconds, there are no exit streams and so concentration of species (at column exit) is zero. Nevertheless, the concentration profiles of the components are due to their affinities and species concentrations in the gas phase. Butene and hydrogen are concentrated near the column exit ($Z/L = 1$), since they have little affinity toward the adsorbent. When the system switches from pressurization/reaction to adsorption/reaction step, butene and hydrogen concentrations increase relatively sharply at the beginning of adsorption. Hydrogen reaches a maximum value and decreases gradually with time. Butadiene and butene concentrations increase with time during high pressure adsorption/reaction step due to a reduction in adsorbent capacity following column regeneration, resulting in lower butene conversion.

The exit concentrations ($Z/L = 0$) of species during the blowdown/reaction step are given at an interval of 250–300 s. Initially, the concentration of butene increases considerably while the concentrations of both butadiene and hydrogen decrease. This indicates that the reaction was reversed for a short period. Then, the concentration of hydrogen increases though the total pressure decreases with time, indicating that the forward reaction occurs. Subsequently, the concentration reduces at the beginning of the step, and butadiene concentration increases gradually with time due to desorption of species from the solid and/or to the forward reaction which is preferred with the reduction in pressure.

During the desorption/reaction step, the reaction continues and results in higher conversion (butene) at lower operating pressure. It is observed that butene is the dominant species during the entire step. The concentration of butadiene increases gradually with time because of desorption and reaction effect.

Figure 5 shows mole fraction distributions of butadiene and butene in the gas-phase along the adsorptive reactor for each step at different times (fractions of step time) during the CSS. During the pressurization step, the pressure inside the bed increases with time from low pressure to high pressure. Hence, two conflicting effects of pressure on the adsorptive reactor is observed. Low pressure is favoured by the reaction but not for the adsorption process and vice versa. Due to this, the mole fraction of butadiene along the bed length is the highest at the beginning of the step and it is decreasing with time as the forward reaction rate decreases and adsorption phenomenon becomes more significant (Fig. 5a). Figure 5b shows that the mole fraction of butene near the

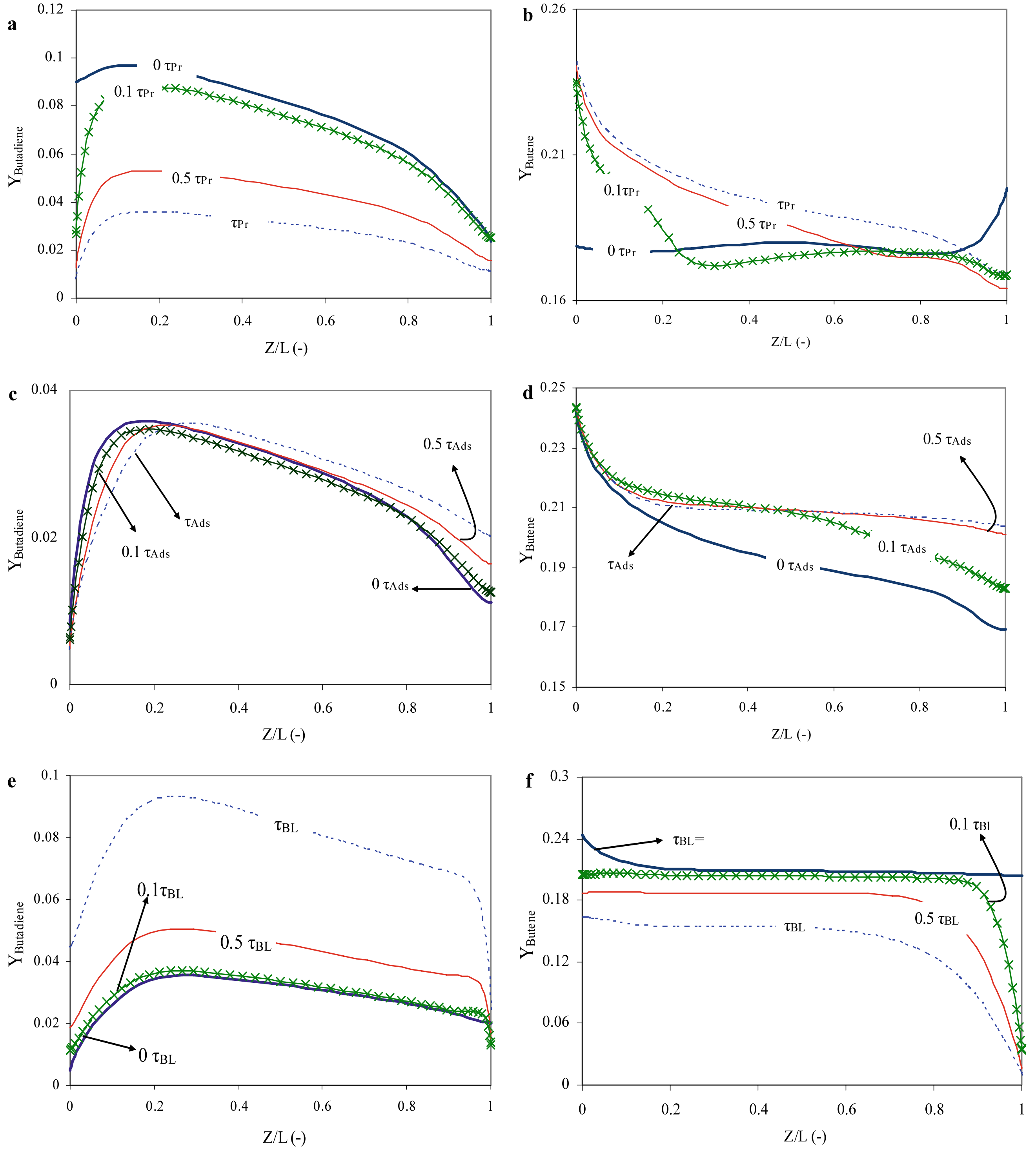

Fig. 5 Axial profiles of the gas-phase mole fraction of butadiene (*left hand side*) and butene (*right hand side*) along the adsorptive length at different times during; (**a**), (**b**): pressurization step; (**c**), (**d**): adsorption step; (**e**), (**f**): blowdown step; (**g**), (**h**): desorption step. (τ_{ads}: adsorption dimensionless step time, τ_{BL}: blowdown dimensionless step time, τ_{Des}: desorption dimensionless step time, and τ_{Pr}: pressurisation dimensionless step time)

feed end increases with time as pressure increases. Butene mole fraction near the product end reached a minimum value at the middle of pressurisation step.

For the adsorption/reaction step, maximum values in the axial profiles of the butadiene can be observed for relative long times (Fig. 5c). The concentration fronts of the buta-

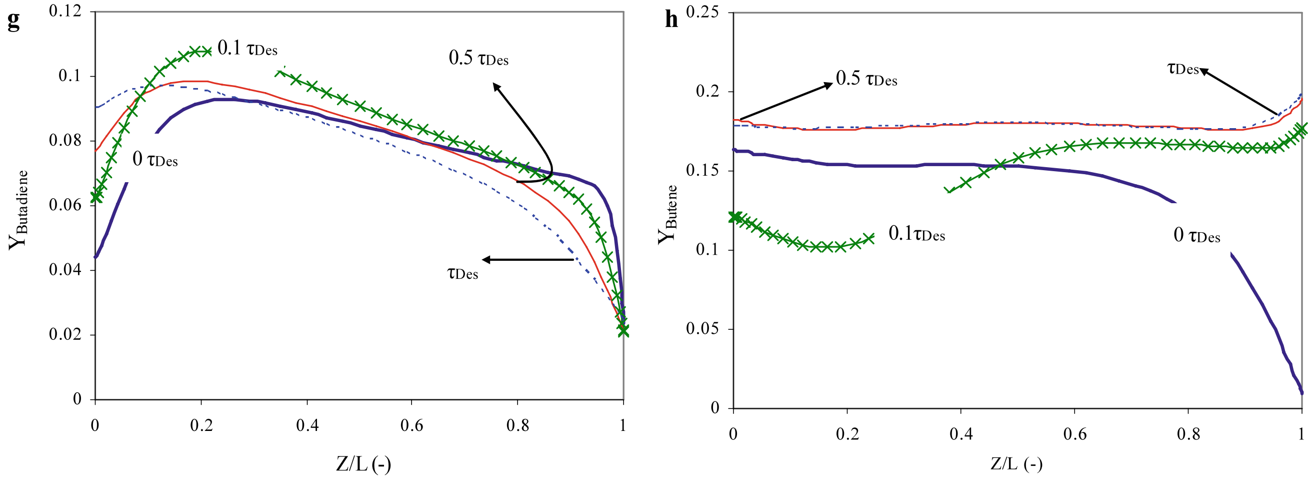

Fig. 5 (*continued*)

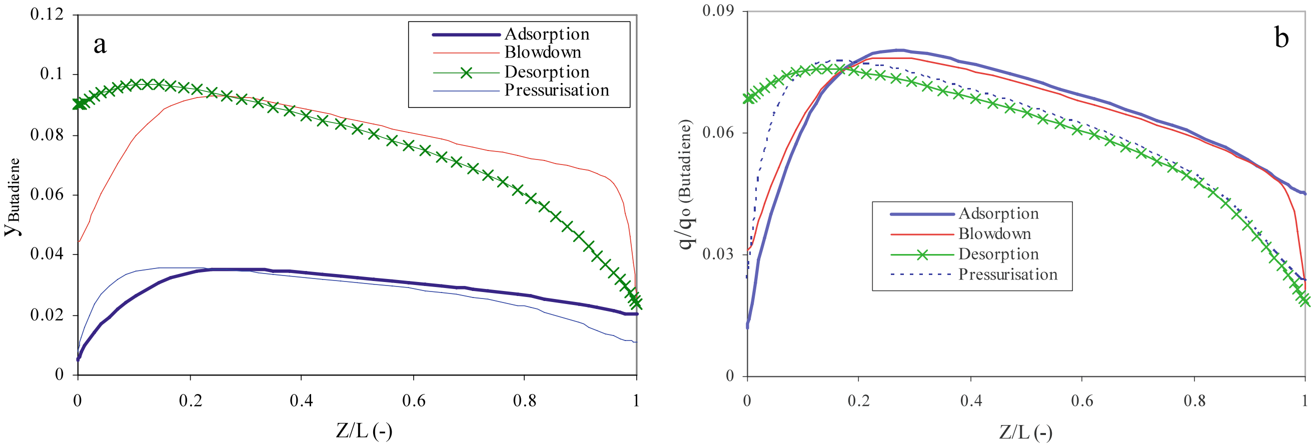

Fig. 6 Mole fraction of butadiene vs. axial distance at the end of each step during CSS; (**a**): in the gas phase, and (**b**): in the solid phase

diene can be seen in the adsorption/reaction step since it is adsorbable. The peak in butadiene mole fraction profile shifted away from the feed end with time, due to the continuous feed of reactant and low conversion of reactant.

In blowdown step, pressure inside the bed decreases with time and, so, total concentration decreases. All species in the gas phase start to leave from the bed open end ($Z/L = 0$). Adsorbable specie starts to desorb out of the solid-phase. The mole fraction of *butene* decreases with time; largely at the closed end of the bed, and slightly at the other end of the bed. However, butene mole fraction increases along the bed. At relative short and medium times, there is a sharp increase in the axial profiles of the butene near the closed end ($Z/L = 1$). However, it is almost constant for the rest of the bed (Fig. 5d). The mole fraction of the butadiene always increases with time inside the bed due to reactant conversion and desorption of its molecules retained in the solid phase with decrease in pressure. This increase is more significant near the opened end of the bed (Fig. 5e).

During desorption step, the mole fraction profiles of butene increases with time except at relatively long times where there is no big change (Fig. 5h). On the other hand, the mole fraction profile of butadiene has different behaviour. In general, it is increasing along the bed in the direction of flow reaching a maximum value near the outlet end (Z/L range between 0.06 and 0.22). However, the higher mole fraction plateaus move out of the bed with time in the direction of flow.

Figures 6a and 6b show the butadiene mole fraction distributions in the gas- and solid-phases along the adsorptive reactor at the end of each step. After the high-pressure adsorption/reaction step, the concentration of butadiene in the gas-phase and, hence, in the solid phase reaches its maximum. During the countercurrent blowdown/reaction step, the reversible reaction and butadiene desorption take place simultaneously, the mole fraction of butadiene in the gas-phase increases (Fig. 6a). However, the concentration of butadiene in the solid-phase decreases slightly, and the distrib-

Table 4 Effect of adsorbent capacity (q_s) of butadiene on PSR performance of 1-butene dehydrogenation

Performance parameters	Component	Step	$q=0.5$	$q=1$	$q=1.25$
Conversion (%)	Butene	All	12.32	16.6	16.9
Purity (%)	Butadiene	Purge	36.2	28.0	27.9
	Hydrogen	Adsorption	12.3	17.1	17.1
Recovery (%)	Butadiene	Purge	64.5	73.8	76.0
	Hydrogen	Adsorption	76.0	64.9	64.3
Yield (%)	Butadiene	All	11.9	16.0	16.4

Table 5 Effect of feed pressure, P_H (atm) on PSR performance of 1-butene dehydrogenation

Performance parameters	Component	Step	$P_H=1.5$	$P_H=3$	$P_H=6$
Conversion (%)	Butene	All	19.5	16.6	15.9
Purity (%)	Butadiene	Purge	19.6	28.0	36.54
	Hydrogen	Adsorption	20.8	17.1	12.3
Recovery (%)	Butadiene	Purge	80.8	73.8	74.2
	Hydrogen	Adsorption	34.7	64.9	74.5
Yield (%)	Butadiene	All	20.0	16.0	12.9

Table 6 Effect of purge pressure, P_L, (atm) on PSR performance of 1-butene dehydrogenation

Performance parameters	Component	Step	$P_L=0.2$	$P_L=0.5$	$P_L=1$
Conversion (%)	Butene	All	25.7	19.3	16.6
Purity (%)	Butadiene	Purge	71.5	47.4	28.0
	Hydrogen	Adsorption	23.3	19.2	17.1
Recovery (%)	Butadiene	Purge	62.3	68.6	73.8
	Hydrogen	Adsorption	84.3	78.2	64.9
Yield (%)	Butadiene	All	24.3	18.7	16.0

ution of butadiene spreads (Fig. 6b). In desorption/reaction step, the reaction is continued and butadiene in the adsorbent is desorbed as well. Near the exit stream ($Z/L=0$) the partial pressure of butadiene at the end of desorption/reaction step is higher than that at the end of adsorption/reaction step. It is obvious from Figs. 6b and 5g that regeneration of the bed is not efficient because of the formation of more butadiene and hence increasing its partial pressure in the bed, specially near bed feed end ($Z/L=1$). The regeneration process of adsorbent can be enhanced in different ways. With Skarstrom cycle, the most two effective methods are either increasing the purge to feed volume ratio (increasing the velocity) and/or using sub-atmospheric pressure during desorption/reaction step.

3.3.3 *Effect of process variables*

Effect of the adsorption capacity q_s: In general, higher adsorption capacity results in better process performance, that is, higher conversion and higher purity and yield for the nonadsorbable material. Nevertheless, both the purity of the adsorbable specie in the purge step and the recovery of nonadsorbable specie in the adsorption step decrease (Table 4).

Feed pressure (atm): 1-butene dehydrogenation is favoured by low pressure. From Table 5 it can be seen that the feed pressure has a great effect on the purity of butadiene in the purge stream. When the pressure of feed increased the separation during the adsorption is better, i.e. greater amount of butadiene is adsorbed. The purity increased by 100% when feed pressure increased from 1.5 to 6 atm. However, butene conversion, yield, hydrogen purity and butadiene recovery decrease with the increase in feed pressure.

Purge pressure (atm): The most important improvement of the vacuum swing reaction (VSR) is the high purity of butadiene in purge stream, high purity and recovery of hydrogen in the adsorption stream, Table 6. This is evidenced by 250% increase in butadiene purity when a sub-atmospheric purge pressure of 0.2 atm is used. In addition, the conversion of butene and product yields increase with lower purge pressures. This is evidenced by the increase in butene conversion

Table 7 Effect of purge-to-feed volume ratio, P/F, on PSR performance of 1-butene dehydrogenation

Performance parameters	Component	Step	$P/F=0.5$	$P/F=1$	$P/F=2$
Conversion (%)	Butene	All	13.4	16.6	21.5
Purity (%)	Butadiene	Purge	27.4	28.0	23.8
	Hydrogen	Adsorption	12.6	17.1	24.8
Recovery (%)	Butadiene	Purge	44.9	73.8	90.8
	Hydrogen	Adsorption	73.2	64.9	37.3
Yield (%)	Butadiene	All	12.62	16.0	20.4

Table 8 Effect of feed composition (y_B, mole fraction) on PSR performance of 1-butene dehydrogenation

Performance parameters	Component	Step	$y_B=0.01$	$y_B=0.10$	$y_B=0.25$	$y_B=0.50$	$y_B=1.00$
Conversion (%)	Butene	All	59.4	25.2	16.6	11.5	6.6
Purity (%)	Butadiene	Purge	59.5	37.8	28.0	20.7	12.3
	Hydrogen	Adsorption	57.0	26.9	17.1	10.9	5.9
Recovery (%)	Butadiene	Purge	73.5	72.7	73.8	73.2	63.7
	Hydrogen	Adsorption	69.7	68.1	64.9	60.5	46.0
Yield (%)	Butadiene	All	59.6	23.9	16.0	11.8	6.0

from 16.6% at 1 atm to 25.7% at 0.2 atm. This represents a significant enhancement in the conversion of butene. However, the recovery of butadiene falls from 73.8% to 62.3%.

Purge-to-feed volume ratio: Table 7 shows the effect of purge-to-feed ration on the performance of PSR. An improvement in recovery of butadiene is observed when the purge/feed ratio is increased from 0.5 to 2. This is due the increase in the amount of butadiene removed from the bed. Clearly, higher P/F ratio resulted in better separation and higher conversion during the adsorption/reaction and very high butadiene recovery, 91%, in the purge step is predicted. However, this is on the expense of butadiene purity and hydrogen recovery.

Feed composition: The effect of butene mole fraction in the feed on butene conversion is shown in Table 8. As expected the dehydrogenation of butene dose not favour the increase in reactant mole fraction. When butene feed composition increases from 0.25 to 1.0, conversion of butene decreases by 60%. Also, purity and recovery of butadiene decrease by 56% and 14% respectively.

3.3.4 Variable reactor configurations with PSR

The effect of bed layering on 1-butene dehydrogenation reaction is to be investigated in this section. Beside the well-mixed bed configuration, four other configurations were studied. The first one is 1/1 layer configuration in which the bed is divided into two equal sections; the first section contains the catalyst and second one contains the adsorbent. The second configuration is the 2/2 layer in which the column is divided into four equal sections; the first contains the catalyst followed by the adsorbent followed by the catalyst followed by the adsorbent. The last two configurations are the 4/4 layer and 8/8 layer. They are similar to 2/2 configuration but more layers of each catalyst and adsorbent were used.

Multilayer arrangements, comprising k separated layers each of catalyst and adsorbent, were considered. The arrangements had similar amount of catalyst and adsorbent and the catalyst to adsorbent volume ratio x_{CA} was kept constant:

$$x_{CA} = \frac{\sum_{i=1}^{k} L_{C,i}{}^{*}(1-\varepsilon_{C,i})^{*}A_{C,i}}{\sum_{i=1}^{k} L_{C,i}{}^{*}(1-\varepsilon_{A,i})^{*}A_{A,i}} \tag{17}$$

Where $L_{C,i}$ and $L_{A,i}$, are the lengths of the catalyst and adsorbent layer i, respectively and A is the cross sectional area of the bed. Since the area A is the same for both layers, and the void fractions in each are not changing within the same type of layer, then the length of layers determines the volume ratio. A value of $x_{CA}=0.50$ was used in our work as the base case. As the number of layers increases, the catalyst-adsorbent bed approaches a homogeneously mixed configuration. With a large number of layers, we approach a well-mixed catalyst/adsorbent distribution in the column.

The effect of layering on the exit molar concentration of butadiene and butene ($y_i C_T$) during the CSS is shown in Figs. 7a and 7b, respectively. In pressurization/reaction step, there are no exit streams and exit concentrations of the species equal to zero. During the adsorption/reaction step, the concentration (mol/m^3) profiles of butadiene increase

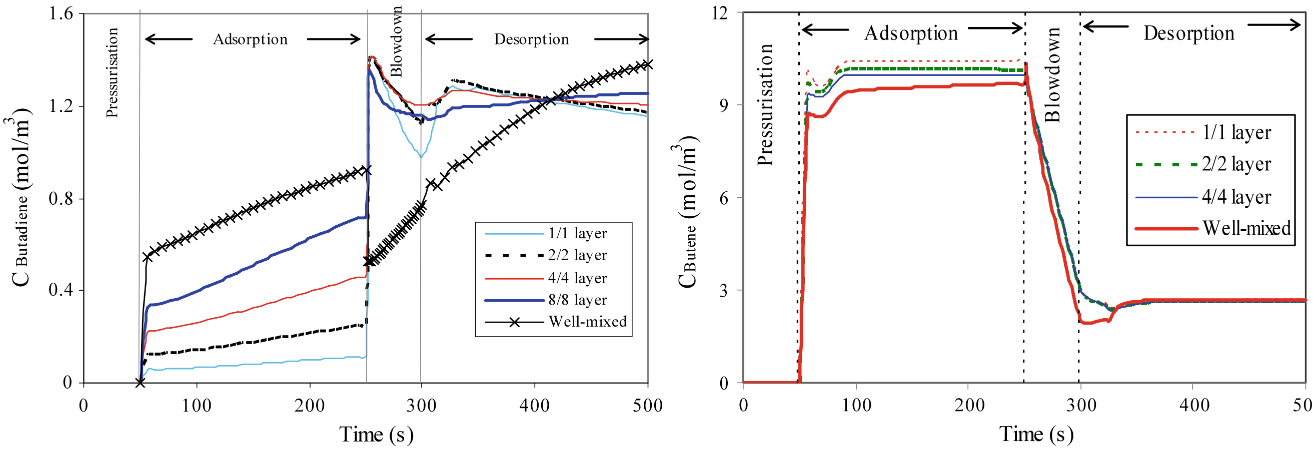

Fig. 7 Concentration profiles with PSR at CSS with variable configurations: (**a**) for butadiene, (**b**) for butene

with time and with the homogeneity of catalyst/adsorbent solids (Fig. 7a). Butene concentration profiles increase sharply at the beginning of the adsorption step and then decreases slightly for a short time before it is increasing again with time because the adsorbent capacity is reduced with time. The conversion of butene at the adsorption/reaction step increases with the increasing in layering, see Fig. 7b.

During the blowdown/reaction step, time between 250–300 s, butadiene concentration profiles change in a way that is not in harmony to the bed configuration especially for configurations far away from the well-mixed configuration. Butadiene concentration profile in the well-mixed configuration, only, increases with time during the blowdown/reaction step while the other configurations profiles behave differently. In $1/1$, $2/2$ and $4/4$ layer configurations, at the beginning of the step, the mole fraction of butadiene is the highest among all configurations. The concentration of species started to decrease as the total pressure and, consequently, total concentration (C_T) inside the column decreases. The increase in butadiene concentration with time in the well-mixed configuration which is opposing the other configurations may due to the reversing of flow and initial concentration of butene in the gas phase at the beginning of the blowdown step and also due to the amount of butadiene adsorbed which is concentrated near the bed feed inlet ($Z/L = 0$). Except the well-mixed configuration, the first section of the bed contains catalyst layer only and the major species in the gas-phase is butene and its concentration is the highest in lower layering configurations because of the low conversion during the adsorption/reaction step. When the flow is reversed, butene moves toward the catalyst section resulting in raising the concentration of butadiene at the beginning of the step.

In desorption/reaction step, 300–500 seconds, butadiene profiles for $1/1$, $2/2$ and $4/4$ configurations increase with time at the beginning of the step and reaching a maximum before they decrease again with time. In $8/8$ configuration, butadiene profile increases very slightly with time. On the other hand, butadiene concentration increases sharply with time in the well-mixed configuration. Nevertheless, the rate of increase at the end of the step is low (see Fig. 7a). The difference in these profiles is due to the initial conditions of the bed in this step and concentration of species, butene, butadiene and hydrogen, in the feed-purging stream.

That the adsorbent regeneration process is affected by bed configuration is observed from comparisons of species concentrations in adsorbent for multi-layer and well mixed configurations (Figs. 8 and 6). For the well-mixed configuration (Fig. 6b), the concentration of butadiene in the solid-phase near the feed input ($Z/L = 0$) at the end of desorption/reaction step is much greater than that at the end of the adsorption step. This is not observed for $1/1$ and $2/2$ configurations (Fig. 8a, b). We also note that for $4/4$ and $8/8$ arrangements, when the adsorbent layer is close to the feed end ($Z/L = 0$), adsorbent regeneration is poor and butadiene is partly adsorbed rather than desorbed (Fig. 8c, d).

Analyses of Table 9 show that the use of PSR for 1-butene dehydrogenation offers several advantages over a fixed bed reactor. First, higher conversion of butene is obtained, close to the equilibrium conversion at low pressure. Higher purities of hydrogen and butadiene are obtained from the adsorption and desorption steps, respectively. Furthermore, Table 9 shows that the hydrogen recovery from the adsorption/reaction step is significantly greater (65%) with a purity of 17% for well-mixed configuration.

Thus, the catalyst/adsorbent configuration has significant effects on the reactor/separator performance. The homogeneous configuration sows good performance as the impacts of separation are enhanced. As the number of layers increases hydrogen recovery is enhanced but at the expense of butadiene recovery which drops from 83.5% to 70.4%. Nevertheless, butadiene purity during desorption/reaction step is not affected significantly. An optimum value of 28.7% is noted with $2/2$ layer configuration.

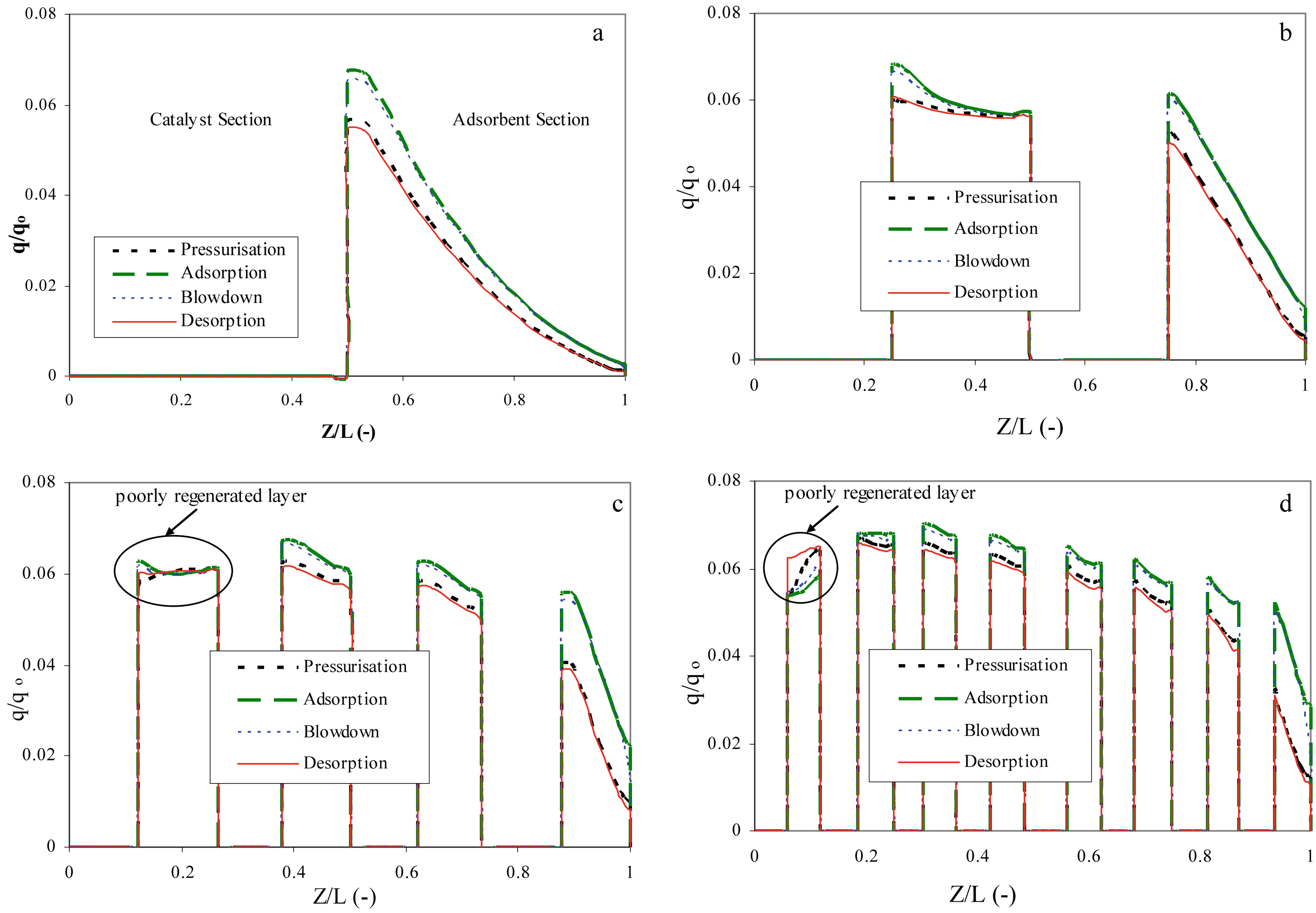

Fig. 8 Butadiene adsorbate concentration vs axial distance at the end of each step during CSS; (**a**): 1/1 layer configuration, (**b**): 2/2 layer configuration, (**c**): 4/4 layer configuration, (**d**): 8/8 layer configuration

Table 9 Effects of distribution of catalyst and adsorbent on the performance of 1-butene dehydrogenation with PSR

Performance parameters	Component	Step	PSR configurations			
			1/1	2/2	4/4	Well-mixed
Conversion (%)	Butene	All	13.1	14.3	15.1	16.7
Purity (%)	Butadiene	Purge	28.2	28.7	28.6	28.0
	Hydrogen	Adsorption	13.1	14.9	15.4	17.1
Recovery (%)	Butadiene	Purge	83.5	81.2	78.1	70.4
	Hydrogen	Adsorption	56.7	58.5	60.1	64.9
Yield (%)	Butadiene, hydrogen	All	13.5	15.1	15.9	16.0

4 Conclusions

A mathematical model to investigate the effects of catalyst/adsorbent distributions on adsorption-enhanced 1-butene dehydrogenation reaction with and without pressure swing effect was developed. The model predictions show that the choice of components to be removed affects reactant conversion in heterogeneous non-elementary reactions. For dehydrogenation of 1-butene, removing 1,3-butadiene results in higher butene conversion than that when hydrogen is removed. Thus, the assumption of elementary reaction kinetics may cause imprecise estimations.

It was noted that by sequentially packing the bed with several layers of catalyst and adsorbent, the reactor bed behaved as reactor/separator in series. Butadiene produced in the first catalyst layer is retained in the intermediate adsorbent layer, thus, increasing the conversion of reactant (butene) and enhancing the reaction rate of the catalyst in layer two. The number of catalyst-adsorbent layers inside the reactor-adsorber unit has an important effect on the purity, recovery and the yield of both butadiene and hydrogen as well as on butene conversion.

For the same catalyst-adsorbent volume ratio and with constant catalyst and adsorbent amounts, the amount of butadiene separated increases with the number of layers. Further, the CSS concentration of the hydrogen in the adsorption/reaction stream increases as well. The reactant conversion is enhanced as a homogeneous arrangement is approached. However, increasing the number of layers results in lower butadiene recovery in the purge step. The regeneration of the bed under the same operating conditions depends, also, on the bed configuration. The closest the adsorbent layer is to the feed end, the poorer is the regeneration of the layer. Desorption pressure was shown to have the highest impact on PSR performance. Thus, the bed regeneration is enhanced and the purity of butadiene increases significantly when VSR is applied.

Although, increasing the number of layers and approach towards homogeneity improves the reactor performance, in practice there are cost implications compared to the simple 1/1 configuration. For example, with a heterogeneous arrangement (when the adsorbent and catalyst are not intimately mixed), the catalyst particles can be readily separated from the adsorbent for the purposes of replacement or additional treatments. Thus, the cost/benefit analysis for heterogeneous and completely homogeneous arrangements must be assessed prior to implementation.

References

Acharya, D.R., Hughes, R.: Modeling of 1-butene dehydrogenation in a fixed bed reactor—bed and pellet profiles. Can. J. Chem. Eng. **68**, 89–96 (1990)

Aida, T., Silveston, P.L.: Cyclic Separating Reactors. Blackwell Publishing, Oxford (2005)

Antonucci, P., Giordano, N., Bart, J.C.J.: Chemical reactions in chromatographic columns. Dehydrogenation of ethane over cadmium-exchanged zeolite 4A. J. Chromatography **150**, 309–317 (1978)

Armor, J.N.: Applications of catalytic inorganic membrane reactors to refinery products. J. Membr. Sci. **147**, 217–233 (1998)

Brito, A., Arvelo, R., Villarroel, R., Garcia, M.T.: Deactivation of a fixed bed Cr2O3/Al2O3 catalyst during butene-1 dehydrogenation, II. Model predictions. React. Kinet. Catal. Lett. **55**, 85–91 (1995)

Carvill, B.T., Hufton, J.R., Anand, M., Sircar, S.: Sorption-enhanced reaction process. AIChE J. **42**, 2765–2772 (1996)

Ding, Y., Alpay, E.: Adsorption-enhanced steam-methane reforming. Chem. Eng. Sci. **55**, 3929–3940 (2000)

Dumez, F.J., Froment, G.F.: Dehydrogenation of 1-butene into butadiene. Kinetics, catalyst coking, and reactor design. Ind. Eng. Chem. Process. Des. Dev. **15**, 291–301 (1976)

Edwards, M.F., Richardson, J.F.: Gas dispersion in packed beds. Chem. Eng. Sci. **23**, 109–123 (1968)

Gomes, V.G.: Enhanced reactor performance with pressure and vacuum swing reaction. Int. J. Chem. React. Eng. **2**, A19 (2004)

Gomes, V.G.: Reactive separation. Ency Chem. Process. 2541–2558 (2005)

Gomes, V.G., Fuller, O.M.: Fixed-bed adsorber dynamics in binary physisorption-diffusion. Can. J. Chem. Eng. **72**, 622–630 (1994)

Gomes, V.G., Fuller, O.M.: Dynamics of propene metathesis: Physisorption and diffusion in heterogeneous catalysis. AIChE J. **42**, 204–213 (1996)

Gomes, V.G., Yee, K.W.K.: A periodic separating reactor for propene metathesis. Chem. Eng. Sci. **57**, 3839–3850 (2002)

Hufton, J.R., Mayorga, S., Sircar, S.: Sorption-enhanced reaction process for hydrogen production. AIChE J. **45**, 248–256 (1999)

Krishna, R.: Reactive separations: more ways to skin a cat. Chem. Eng. Sci. **57**, 1491–1504 (2002)

Lu, Z.P., Rodrigues, A.E.: Simulation of pressure swing adsorption reactors. In: CHEMPOR'93, International Chem. Eng. Conf, Porto, Portugal, Apr. 4–6 (1993)

Lu, Z.P., Rodrigues, A.E.: Pressure swing adsorption reactors: simulation of three-step one-bed process. AIChE J. **40**, 1118–1137 (1994)

Malek, A., Farooq, S.: Study of a six-bed pressure swing adsorption process. AIChE J. **43**, 2509–2523 (1997)

Rawadieh, S., Gomes, V.G.: Catalyst-adsorbent configurations in enhancing adsorptive reactor performance. Int. J. Chem. React. Eng. **5**, A108 (2007)

Reid, R.C., Prausnitz, J.M., Poling, B.E.: The Properties of Gases and Liquids. New York, McGraw-Hill (1987)

Ruthven, D.M., Farooq, S., Knaebel, K.S.: Pressure Swing Adsorption. New York, VCH (1994)

Schweich, D., Villermaux, J.: Model for catalytic dehydrogenation of cyclohexane in a chromatographic reactor: comparison of theory and experiment. Ind. Eng. Chem. Fundam. **21**, 47–51 (1982)

Sereno, C., Rodrigues, A.: Can steady-state momentum equations be used in modelling pressurization of adsorption beds? Gas Sep. Purif. **7**, 167–174 (1993)

Sheikh, J., Kershenbaum, L.S., Alpay, E.: 1-butene dehydrogenation in rapid pressure swing reaction processes. Chem. Eng. Sci. **56**, 1511–1516 (2001)

Stankiewicz, A.: Reactive separations for process intensification: an industrial perspective. Chem. Eng. Process. **42**, 137–144 (2003)

Stankiewicz, A.I., Moulijn, J.A.: Process intensification: transforming chemical engineering. Chem. Eng. Prog. **96**, 22–34 (2000)

Ullmann, F.: Ullmann's Encyclopedia of Industrial Chemistry, 7th ed. New York, Wiley (2007)

Vaporciyan, G.G., Kadlec, R.H.: Equilibrium-limited periodic separating reactors. AIChE J. **33**, 1334–1343 (1987)

William, A., Kulprathipanja, S.: Reactive separation processes. In: Kulprathipanja, S. (ed.) Reactive Separation Processes. Taylor & Francis, New York (2002)

Xiu, G.-h., Li, P., Rodrigues, A.E.: Sorption-enhanced reaction process with reactive regeneration. Chem. Eng. Sci. **57**, 3893–3908 (2002a)

Xiu, G.-h., Soares, J.L., Li, P., Rodrigues, A.E.: Simulation of five-step one-bed sorption-enhanced reaction process. AIChE J. **48**, 2817–2832 (2002b)

Yongsunthon, I., Alpay, E.: Conversion-temperature trajectories for well-mixed adsorptive reactors. Chem. Eng. Sci. **53**, 691–696 (1998a)

Yongsunthon, I., Alpay, E.: Design and optimisation of temperature cycled adsorptive reactors. Comput. Chem. Eng. **22**, S733–S736 (1998b)